GEOPHYSICS, VOL. 51, NO. 10 (OCTOBER 1986); P. 1954–1966, 5 FIGS., 1 TABLE.

Weak elastic anisotropy

Leon Thomsen*

ABSTRACT

Most bulk elastic media are weakly anisotropic. The equations governing weak anisotropy are much simpler than those governing strong anisotropy, and they are much easier to grasp intuitively. These equations indicate that a certain anisotropic parameter (denoted δ) controls most anisotropic phenomena of importance in exploration geophysics, some of which are nonnegligible even when the anisotropy is weak. The critical parameter δ is an awkward combination of elastic parameters, a combination which is totally independent of horizontal velocity and which may be either positive or negative in natural contexts.

INTRODUCTION

In most applications of elasticity theory to problems in petroleum geophysics, the elastic medium is assumed to be isotropic. On the other hand, most crustal rocks are found experimentally to be anisotropic. Further, it is known that if a layered sequence of different media (isotropic or not) is probed with an elastic wave of wavelength much longer than the typical layer thickness (i.e., the normal seismic exploration context), the wave propagates as though it were in a homogeneous, but anisotropic, medium (Backus, 1962). Hence, there is a fundamental inconsistency between practice on the one hand and reality on the other.

Two major reasons for the continued existence of this inconsistency come readily to mind:

(1) The most commonly occurring type of anisotropy (transverse isotropy) masquerades as isotropy in near-vertical reflection profiling, with the angular dependence disguised in the uncertainty of the depth to each reflector (cf., Krey and Helbig, 1956).

(2) The mathematical equations for anisotropic wave propagation are algebraically daunting, even for this simple case.

The purpose of this paper is to point out that in most cases of interest to geophysicists the anisotropy is weak (10–20 percent), allowing the equations to simplify considerably. In fact, the equations become so simple that certain basic conclusions are immediately obvious:

(1) The most common measure of anisotropy (contrasting vertical and horizontal velocities) is not very relevant to problems of near-vertical P-wave propagation.

(2) The most critical measure of anisotropy (denoted δ) does not involve the horizontal velocity at all in its definition and is often undetermined by experimental programs intended to measure anisotropy of rock samples.

(3) A common approximation used to simplify the anisotropic wave-velocity equations (elliptical anisotropy) is usually inappropriate and misleading for P- and SV-waves.

(4) Use of Poisson's ratio, as determined from vertical P and S velocities, to estimate horizontal stress usually leads to significant error.

These conclusions apply irrespective of the physical cause of the anisotropy. Specifically, anisotropy in sedimentary rock sequences may be caused by preferred orientation of anisotropic mineral grains (such as in a massive shale formation), preferred orientation of the shapes of isotropic minerals (such as flat-lying platelets), preferred orientation of cracks (such as parallel cracks, or vertical cracks with no preferred azimuth), or thin bedding of isotropic or anisotropic layers. The conclusions stated here may be applied to rocks with any or all of these physical attributes, with the sole restriction that the resulting anisotropy is "weak" (this condition is given precise meaning below).

To establish these conclusions, some elementary facts about anisotropy are reviewed in the next section. This is followed by a presentation of the simplified angular dependence of wave velocities appropriate for weak anisotropy. In the following section, the anisotropic parameters thus identified are used to analyze several common problems in petroleum geophysics. Finally, further discussion and conclusions are presented.

REVIEW OF ELASTIC ANISOTROPY

A linearly elastic material is defined as one in which each component of stress σ_{ij} is linearly dependent upon every component of strain $\varepsilon_{k\ell}$ (Nye, 1957). Since each directional index may assume values of 1, 2, 3 (representing directions x, y, z),

Manuscript received by the Editor September 9, 1985; revised manuscript received February 24, 1986.
*Amoco Production Company, P.O. Box 3385, Tulsa, OK 74102.

there are nine such relations, each involving one component of stress and nine components of strain. These nine equations may be written compactly as

$$\sigma_{ij} = \sum_{k=1}^{3} \sum_{\ell=1}^{3} \mathbf{C}_{ijk\ell} \varepsilon_{k\ell}, \; i, j = 1, 2, 3, \tag{1}$$

where the $3 \times 3 \times 3 \times 3$ elastic modulus tensor $\mathbf{C}_{ijk\ell}$ completely characterizes the elasticity of the medium. Because of the symmetry of stress ($\sigma_{ij} = \sigma_{ji}$), only six of these equations are independent. Because of the symmetry of strain ($\varepsilon_{k\ell} = \varepsilon_{\ell k}$), only six of the terms on the right side of each set of equations (1) are independent.

Hence, without loss of generality, the elasticity may be represented more compactly with a change of indices, following the Voigt recipe:

$$\begin{array}{cccccccccc} ij \text{ or } k\ell & : & 11 & 22 & 33 & 32=23 & 31=13 & 12=21 & & \\ \downarrow & \downarrow & \downarrow & \downarrow & \downarrow & \downarrow & \downarrow & \downarrow & , & (2) \\ \alpha & \beta & 1 & 2 & 3 & 4 & 5 & 6 & & \end{array}$$

so that the $3 \times 3 \times 3 \times 3$ tensor $\mathbf{C}_{ijk\ell}$ may be represented by the 6×6 matrix $\mathbf{C}_{\alpha\beta}$. Each symmetry class has its own pattern of nonzero, independent components $\mathbf{C}_{\alpha\beta}$. For example, for isotropic media the matrix assumes the simple form

$$\mathbf{C}_{\alpha\beta} = \begin{bmatrix} C_{33} & (C_{33} - 2C_{44}) & (C_{33} - 2C_{44}) & & & \\ & C_{33} & (C_{33} - 2C_{44}) & & & \\ & & C_{33} & & & \\ & & & C_{44} & & \\ & & & & C_{44} & \\ & & & & & C_{44} \end{bmatrix} \ldots \text{isotropy}. \tag{3}$$

Only the nonzero components in the upper triangle are shown; the lower triangle is symmetrical. These components are related to the Lamé parameters λ and μ and to the bulk modulus K by

$$C_{33} = \lambda + 2\mu = K + \tfrac{4}{3}\mu;$$

and (4)

$$C_{44} = \mu.$$

The simplest anisotropic case of broad geophysical applicability has one distinct direction (usually, but not always, vertical), while the other two directions are equivalent to each other. This case—called transverse isotropy, or hexagonal symmetry—is the only one considered explicitly here (although the present approach is useful for any symmetry). Hence, subsequent use of the term "anisotropy" refers only to this particular case.

The elastic modulus matrix has five independent components among twelve nonzero components, giving the elastic modulus matrix the form

$$\mathbf{C}_{\alpha\beta} = \begin{bmatrix} C_{11} & (C_{11} - 2C_{66}) & C_{13} & & & \\ & C_{11} & C_{13} & & & \\ & & C_{33} & & & \\ & & & C_{44} & & \\ & & & & C_{44} & \\ & & & & & C_{66} \end{bmatrix} \ldots \text{transverse isotropy}, \tag{5}$$

where the three-direction (z) is taken as the unique axis. It is significant that the generalization from isotropy to anisotropy introduces three new elastic moduli, rather than just one or two. (If the physical cause of the anisotropy is known, e.g., thin layering of certain isotropic media, these five moduli may not be independent after all. However, since the physical cause is rarely determined, the general treatment is followed here.) A comparison of the isotropic matrix, equation (3), with the anisotropic matrix, equation (5), shows how the former is a degenerate special case of the latter, with

$$\left.\begin{array}{ll} C_{11} \to C_{33} & (6a) \\ C_{66} \to C_{44} & (6b) \\ C_{13} \to C_{33} - 2C_{44} & (6c) \end{array}\right\} \ldots \text{isotropy}.$$

The elastic modulus matrix $\mathbf{C}_{\alpha\beta}$ in equation (5) may be used to reconstruct the tensor $\mathbf{C}_{ijk\ell}$ using equation (2), so that the constitutive relation in equation (1) is known for the anisotropic medium.

The relation may be used in the equation of motion (e.g., Daley and Hron, 1977; Keith and Crampin, 1977a, b, c), yielding a wave equation. There are three independent solutions—one quasi-longitudinal, one transverse, and one quasi-transverse—for each direction of propagation. The three are polarized in mutually orthogonal directions. The exactly transverse wave has a polarization vector with no component in the three-direction. It is denoted by SH; the other vector is denoted by SV. Daley and Hron (1977) give a clear derivation of the directional dependence of the three phase velocities:

$$\rho v_P^2(\theta) = \frac{1}{2}\left[C_{33} + C_{44} + (C_{11} - C_{33})\sin^2\theta + D(\theta)\right]; \tag{7a}$$

$$\rho v_{SV}^2(\theta) = \frac{1}{2}\left[C_{33} + C_{44} + (C_{11} - C_{33})\sin^2\theta - D(\theta)\right]; \tag{7b}$$

and

$$\rho v_{SH}^2(\theta) = C_{66}\sin^2\theta + C_{44}\cos^2\theta, \tag{7c}$$

where ρ is density and phase angle θ is the angle between the wavefront normal and the unique (vertical) axis (Figure 1).

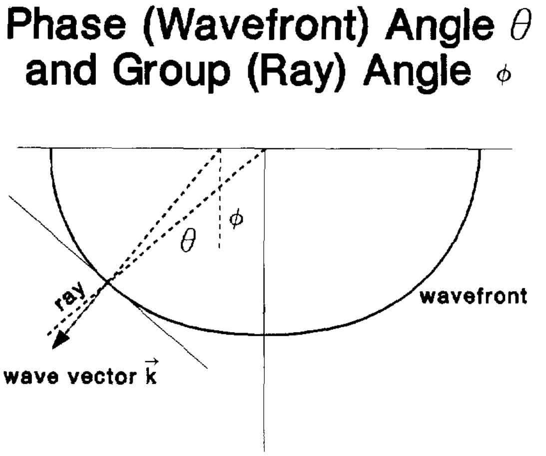

FIG. 1. This figure graphically indicates the definitions of phase (wavefront) angle and group (ray) angle.

$D(\theta)$ is compact notation for the quadratic combination:

$$D(\theta) \equiv \Big\{ (C_{33} - C_{44})^2 + 2\Big[2(C_{13} + C_{44})^2 - (C_{33} - C_{44})(C_{11} + C_{33} - 2C_{44})\Big]\sin^2\theta + \Big[(C_{11} + C_{33} - 2C_{44})^2 - 4(C_{13} + C_{44})^2\Big]\sin^4\theta\Big\}^{1/2} \tag{7d}$$

(note misprint in the corresponding expression in Daley and Hron, 1977). It is the algebraic complexity of D which is a primary obstacle to use of anisotropic models in analyzing seismic exploration data.

It is useful to recast equations (7a)–(7d) (involving five elastic moduli) using notation involving only two elastic moduli (or equivalently, vertical P- and S-wave velocities) plus three measures of anisotropy. These three "anisotropies" should be appropriate combinations of elastic moduli which (1) simplify equations (7); (2) are nondimensional, so that one may speak of X percent P anisotropy, etc.; and (3) reduce to zero in the degenerate case of isotropy, as indicated by relations (6), so that materials with small values ($\ll 1$) of "anisotropy" may be denoted "weakly anisotropic."

Some suitable combinations are suggested by the form of equations (7):

$$\varepsilon \equiv \frac{C_{11} - C_{33}}{2C_{33}}; \tag{8a}$$

$$\gamma \equiv \frac{C_{66} - C_{44}}{2C_{44}}; \tag{8b}$$

and

$$\delta^* \equiv \frac{1}{2C_{33}^2}\Big[2(C_{13} + C_{44})^2 - (C_{33} - C_{44})(C_{11} + C_{33} - 2C_{44})\Big]. \tag{8c}$$

The utility of the factors of two in definitions (8a)–(8d) will be evident shortly. The definition of equation (8c) is not unique, and it may be justified only as in the case considered next, where it leads eventually to simplification. The vertical sound speeds for P- and S-waves are, respectively,

$$\alpha_0 = \sqrt{C_{33}/\rho}; \tag{9a}$$

and

$$\beta_0 = \sqrt{C_{44}/\rho}. \tag{9b}$$

Then, equations (7) become (exactly)[1]

$$v_P^2(\theta) = \alpha_0^2\Big[1 + \varepsilon \sin^2\theta + D^*(\theta)\Big]; \tag{10a}^*$$

$$v_{SV}^2(\theta) = \beta_0^2\Big[1 + \frac{\alpha_0^2}{\beta_0^2}\varepsilon \sin^2\theta - \frac{\alpha_0^2}{\beta_0^2}D^*(\theta)\Big]; \tag{10b}^*$$

$$v_{SH}^2(\theta) = \beta_0^2\Big[1 + 2\gamma \sin^2\theta\Big], \tag{10c}^*$$

with

$$D^*(\theta) \equiv \frac{1}{2}\left(1 - \frac{\beta_0^2}{\alpha_0^2}\right)\left\{\left[1 + \frac{4\delta^*}{(1 - \beta_0^2/\alpha_0^2)^2}\sin^2\theta\cos^2\theta + \frac{4(1 - \beta_0^2/\alpha_0^2 + \varepsilon)\varepsilon}{(1 - \beta_0^2/\alpha_0^2)^2}\sin^4\theta\right]^{1/2} - 1\right\}. \tag{10d}^*$$

Before considering the case of weak anisotropy, it is important to clarify the distinction between the phase angle θ and the ray angle ϕ (along which energy propagates). Referring to Figure 1, the wavefront is locally perpendicular to the propagation vector **k**, since **k** points in the direction of maximum rate of increase in phase. The phase velocity $v(\theta)$ is also called the wavefront velocity, since it measures the velocity of advance of the wavefront along $\mathbf{k}(\theta)$. Since the wavefront is nonspherical, it is clear that θ (also called the wavefront-normal angle) is different from ϕ, the ray angle from the source point to the wavefront. Following Berryman (1979), these relationships may be stated (for each wave type) in terms of the wave vector

$$\mathbf{k} = k_x \hat{\mathbf{x}} + k_z \hat{\mathbf{z}}, \tag{11}^*$$

where the components are clearly

$$k_x = k(\theta)\sin\theta; \tag{11a}^*$$

$$k_z = k(\theta)\cos\theta; \tag{11b}^*$$

and

$$k_y = 0;$$

and the scalar length is

$$k(\theta) = \sqrt{k_x^2 + k_z^2} = \omega/v(\theta), \tag{11c}^*$$

where ω is angular frequency. The ray velocity **V** is then given

[1]This, and other expressions below which are marked with an asterisk are valid for arbitrary (not just weak) anisotropy.

by

$$\mathbf{V} = \frac{\partial(kv)}{\partial k_x}\hat{\mathbf{x}} + \frac{\partial(kv)}{\partial k_z}\hat{\mathbf{z}}, \qquad (12)^*$$

where the partial derivatives are taken with the other component of $\mathbf{k}$ held constant. Because of the similarity in form between equation (12) and the usual expression for group velocity in a dispersive medium, $\mathbf{V}$ is also called the group velocity and ϕ is the group angle. From Figure 1, ϕ is given by

$$\tan\left(\phi(\theta)\right) = \frac{\partial kv}{\partial k_x}\Big/\frac{\partial kv}{\partial k_z} \qquad (13a)^*$$

$$= \left(v\sin\theta + \frac{dv}{d\theta}\cos\theta\right)\Big/\left(v\cos\theta - \frac{dv}{d\theta}\sin\theta\right)$$

$$= \left(\tan\theta + \frac{1}{v}\frac{dv}{d\theta}\right)\Big/\left(1 - \frac{\tan\theta}{v}\frac{dv}{d\theta}\right). \qquad (13b)^*$$

Berryman (1979) also shows that the scalar magnitude V of the group velocity is given in terms of the phase velocity magnitude v by

$$V^2\left(\phi(\theta)\right) = v^2(\theta) + \left(\frac{dv}{d\theta}\right)^2. \qquad (14)^*$$

At $\theta = 0$ degrees and $\theta = 90$ degrees, the second term in equation (14) vanishes, so that for these extreme angles (vertical and horizontal propagation, respectively), group velocity equals phase velocity.

WEAK ANISOTROPY

All the results of the previous section are exact, given equations (1) and (5). However, the algebraic complexity of equations (10) impedes a clear understanding of their physical content. Progress may be made, however, by observing that most rocks are only weakly anisotropic, even though many of their constituent minerals are highly anisotropic.

Table 1 presents data on anisotropy for a number of sedimentary rocks. The original data consist (in the laboratory cases) of ultrasonic velocity measurements or (in the field cases) of seismic-band velocity measurements. These data were interpreted by the original investigators in terms of the five elastic moduli of transverse isotropy. In Table 1, these moduli are recast in terms of the vertical velocities α_0, and β_0, and the three anisotropies ε, δ^*, and γ defined above. Also, a fourth measure of anisotropy (δ, defined below as a more useful alternative to δ^*) is shown. As seen in the table, these quantities provide an immediate estimate of the three types of anisotropy that are unavailable by simple inspection of the moduli themselves. Table 1 confirms that most of these rocks have anisotropy in the weak-to-moderate range (i.e., <0.2), as expected. The table also shows data for some common crystalline minerals (which in some cases are strongly anisotropic) and for some layered composites.

The listing of measurements of sedimentary rock anisotropy in Table 1 from the literature is nearly exhaustive. However, perhaps twice as many partial studies of anisotropy (measuring vertical and horizontal P and S velocities) have appeared. It is clear that the requisite five parameters may not be obtained from four measurements (at least one measurement at an oblique angle, preferably 45 degrees, is required). As is shown below, this omitted datum is the most important one for most applications in petroleum geophysics. Hence, these partial studies are omitted from Table 1.

In addition to intrinsic anisotropy, one must consider extrinsic anisotropy, for example, due to fine layering of isotropic beds. Many examples could be listed, but it is not clear how to pick representative examples. This table has been limited to the particular examples defined by Levin (1979) (these choices are discussed further below).

With Table 1 as justification of the approximation of weak anisotropy, it now makes sense to expand equations (10) in a Taylor series in the small parameters ε, δ^*, and γ at fixed θ. Retaining only terms linear in these small parameters, the quadratic D^* is approximately

$$D^* \approx \frac{\delta^*}{(1 - \beta_0^2/\alpha_0^2)}\sin^2\theta\cos^2\theta + \varepsilon\sin^4\theta. \qquad (15)$$

Substituting this expression into equations (10a) and (10b) and further linearizing yields a final set of phase velocities that is valid for weak anisotropy:

$$v_p(\theta) = \alpha_0(1 + \delta\sin^2\theta\cos^2\theta + \varepsilon\sin^4\theta), \qquad (16a)$$

$$v_{SV}(\theta) = \beta_0\left[1 + \frac{\alpha_0^2}{\beta_0^2}(\varepsilon - \delta)\sin^2\theta\cos^2\theta\right], \qquad (16b)$$

and

$$v_{SH}(\theta) = \beta_0(1 + \gamma\sin^2\theta). \qquad (16c)$$

Equations (16) display the required simplicity of form. They have been arranged so that, for small angles θ, each successive term contributes to the total by successively smaller orders of magnitude. This relation leads to replacement of the (initially defined) anisotropy parameter δ^* in equation (8c) by

$$\delta \equiv \frac{1}{2}\left[\varepsilon + \frac{\delta^*}{(1 - \beta_0^2/\alpha_0^2)}\right]$$

$$= \frac{(C_{13} + C_{44})^2 - (C_{33} - C_{44})^2}{2C_{33}(C_{33} - C_{44})}. \qquad (17)^*$$

The parameter δ^* is not required further.

From Table 1, note that all three anisotropies ε, δ, and γ are usually of the same order of magnitude. Because of this, it is clear from equation (16a) that at small angles θ where $\sin^2\cos^2$ is not nearly as small as $\sin^4$, the second term (in δ) is not nearly as small as the last term (in ε). It is in this regime (small θ) where most reflection profiling takes place. Hence this δ term will dominate most anisotropic effects in this context, unless $\varepsilon \gg \delta$ in some particular case.

The trigonometric factor $\cos^2\theta$ in the second term of equation (16a) rather than $(1 - \sin^2\theta)$ appears by design. This factor ensures that the angular dependence of $v_p(\theta)$, at near-horizontal propagation, is clearly dominated by ε (since $\cos\pi/2 = 0$), just as the near-vertical propagation is dominated by δ. In fact, at horizontal incidence,

$$v_p(\pi/2) = \alpha_0(1 + \varepsilon). \qquad (18a)$$

Since α_0 is the vertical P velocity, it is now abundantly clear

Table 1. Measured anisotropy in sedimentary rocks. This table compiles and condenses virtually all published data on anisotropy of sedimentary rocks, plus some related materials.

Sample	Conditions	V_p (f/s) (m/s)	V_s (f/s) (m/s)	ε	δ^*	δ	γ	ρ(g/cm^3)
Taylor[1] sandstone	P_{eff} = 0 MPa, saturated	11 050 3 368	6 000 1 829	0.110	−0.127	−0.035	0.255	2.500
Mesaverde (4903)[2] mudshale	P_{eff} = 27.58 MPa satd, undrnd	14 860 4 529	8 869 2 703	0.034	0.250	0.211	0.046	2.520
Mesaverde (4912)[2] immature sandstone	P_{eff} = 27.58 MPa satd, undrnd	14 684 4 476	9 232 2 814	0.097	0.051	0.091	0.051	2.500
Mesaverde (4946)[2] immature sandstone	P_{eff} = 27.58 MPa satd, undrnd	13 449 4 099	7 696 2 346	0.077	−0.039	0.010	0.066	2.450
Mesaverde (5469.5)[2] silty limestone	P_{eff} = 27.58 MPa satd, undrnd	16 312 4 972	9 512 2 899	0.056	−0.041	−0.003	0.067	2.630
Mesaverde (5481.3)[2] immature sandstone	P_{eff} = 27.58 MPa satd, undrnd	14 270 4 349	8 434 2 571	0.091	0.134	0.148	0.105	2.460
Mesaverde (5501)[2] clayshale	P_{eff} = 27.58 MPa satd, undrnd	12 887 3 928	6 742 2 055	0.334	0.818	0.730	0.575	2.590
Mesaverde (5555.5)[2] immature sandstone	P_{eff} = 27.58 MPa satd, undrnd	14 891 4 539	8 877 2 706	0.060	0.147	0.143	0.045	2.480
Mesaverde (5566.3)[2] laminated siltstone	P_{eff} = 27.58 MPa satd, undrnd	14 596 4 449	8 482 2 585	0.091	0.688	0.565	0.046	2.570
Mesaverde (5837.5)[2] immature sandstone	P_{eff} = 27.58 MPa satd, undrnd	15 327 4 672	9 294 2 833	0.023	−0.013	0.002	0.013	2.470
Mesaverde (5858.6)[2] clayshale	P_{eff} = 27.58 MPa satd, undrnd	12 448 3 794	6 804 2 074	0.189	0.154	0.204	0.175	2.560
Mesaverde (6423.6)[2] calcareous sandstone	P_{eff} = 27.58 MPa satd, undrnd	17 914 5 460	10 560 3 219	0.000	−0.345	−0.264	−0.007	2.690
Mesaverde (6455.1)[2] immature sandstone	P_{eff} = 27.58 MPa satd, undrnd	14 496 4 418	8 487 2 587	0.053	0.173	0.158	0.133	2.450
Mesaverde (6542.6)[2] immature sandstone	P_{eff} = 27.58 MPa satd, undrnd	14 451 4 405	8 339 2 542	0.080	−0.057	−0.003	0.093	2.510
Mesaverde (6563.7)[2] mudshale	P_{eff} = 27.58 MPa satd, undrnd	16 644 5 073	9 837 2 998	0.010	0.009	0.012	−0.005	2.680
Mesaverde (7888.4)[2] sandstone	P_{eff} = 27.58 MPa satd, undrnd	15 973 4 869	9 549 2 911	0.033	0.030	0.040	−0.019	2.500
Mesaverde (7939.5)[2] mudshale	P_{eff} = 27.58 MPa satd, undrnd	14 096 4 296	8 106 2 471	0.081	0.118	0.129	0.048	2.660

[1]Rai and Frisillo, 1982
[2]Kelley, 1983 (number in parentheses is depth label)

Table 1. Continued

Sample	Conditions	V_P (f/s) (m/s)	V_S (f/s) (m/s)	ε	δ*	δ	γ	ρ(g/cm³)
Mesaverde shale (350)[3]	P_{eff} = 20.00 MPa dry	11 100 3 383	8 000 2 438	0.065	−0.003	0.059	0.071	2.35
Mesaverde sandstone (1582)[3]	P_{eff} = 20.00 MPa dry	12 100 3 688	9 100 2 774	0.081	0.010	0.057	0.000	2.73
Mesaverde shale (1599)[3]	P_{eff} = 20.00 MPa dry	12 800 3 901	8 800 2 682	0.137	−0.078	−0.012	0.026	2.64
Mesaverde sandstone (1958)[3]	P_{eff} = 50.00 MPa dry	13 900 4 237	9 900 3 018	0.036	−0.037	−0.039	0.030	2.69
Mesaverde shale (1968)[3]	P_{eff} = 50.00 MPa dry	15 900 4 846	10 400 3 170	0.063	−0.031	0.008	0.028	2.69
Mesaverde sandstone (3512)[3]	P_{eff} = 50.00 MPa dry	15 200 4 633	10 600 3 231	−0.026	−0.004	−0.033	0.035	2.71
Mesaverde shale (3511)[3]	P_{eff} = 50.00 MPa dry	14 300 4 359	10 000 3 048	0.172	−0.088	0.000	0.157	2.81
Mesaverde sandstone (3805)[3]	P_{eff} = 20.00 MPa dry	13 000 3 962	9 600 2 926	0.055	−0.066	−0.089	0.041	2.87
Mesaverde shale (3883)[3]	P_{eff} = 50.00 MPa dry	12 300 3 749	8 600 2 621	0.128	−0.025	0.078	0.100	2.92
Dog Creek[4] shale	in situ, z = 143.3 m (430 ft)	6 150 1 875	2 710 826	0.225	−0.020	0.100	0.345	2.000
Wills Point[4] shale	in situ, z = 58.3 m (175 ft)	3 470 1 058	1 270 387	0.215	0.359	0.315	0.280	1.800
	P_{eff} = 0, satd, undrnd	13 550 4 130	7 810 2 380	0.085	0.104	0.120	0.185	2.640
Cotton Valley[5] shale	P_{eff} = 111.70 MPa satd, undrnd	15 490 4 721	9 480 2 890	0.135	0.172	0.205	0.180	2.640
Pierre[6] shale	in situ, z = 450 m	6 804 2 074	2 850 869	0.110	0.058	0.090	0.165	2.25?
	in situ, z = 650 m	6 910 2 106	2 910 887	0.195	0.128	0.175	0.300	2.25?
	in situ, z = 950 m	7 224 2 202	3 180 969	0.015	0.085	0.060	0.030	2.25?
shale (5000)[7]	P_c = 0, satd, undrnd	10 000 3 048	4 890 1 490	0.255	−0.270	−0.050	0.480	2.420

[3]Lin, 1985 (number in parentheses is depth label)
[4]Robertson and Corrigan, 1983
[5]Tosaya, 1982
[6]White, et al., 1982
[7]Jones and Wang, 1981 (depth of core shown)

Table 1. Continued

Sample	Conditions	V_P (f/s) (m/s)	V_S (f/s) (m/s)	ε	δ*	δ	γ	ρ(g/cm³)
	P_c = 101.36 MPa satd, undrnd	11 080 3 377	4 890 1 490	0.200	-0.282	-0.075	0.510	2.420
Oil Shale[8]	unknown	13 880 4 231	8 330 2 539	0.200	0.000	0.100	0.145	2.370
Green River[9] shale	P_c = 0, satd, undrnd	13 670 4 167	7 980 2 432	0.040	-0.013	0.010	0.030	2.310
	P_c = 68.95 MPa, satd, undrnd	14 450 4 404	8 470 2 582	0.025	0.056	0.055	0.020	2.310
Berea[10] sandstone	P_{eff} = 68.95 Mpa, saturated	13 800 4 206	8 740 2 664	0.002	0.023	0.020	0.005	2.140
Bandera[10] sandstone	P_{eff} = 68.95 Mpa, saturated	12 500 3 810	7 770 2 368	0.030	0.037	0.045	0.030	2.160
Green River[11] shale	P_c = 202.71 MPa, air dry	10 800 3 292	5 800 1 768	0.195	-0.45	-0.220	0.180	2.075
Lance[11] sandstone	P_c = 202.71 Mpa, air dry	16 500 5 029	9 800 2 987	-0.005	-0.032	-0.015	0.005	2.430
Ft. Union[11] siltstone	P_c = 202.71 Mpa, air dry	16 000 4 877	9 650 2 941	0.045	-0.071	-0.045	0.040	2.600
Timber Mtn[11] tuff	P_c = 202.71 Mpa, air dry	15 900 4 846	6 090 1 856	0.020	-0.003	-0.030	0.105	2.330
Muscovite[12] crystal	P_c = 0	14 500 4 420	6 860 2 091	1.12	-1.23	-0.235	2.28	2.79
Quartz crystal[12] (hexag. approx.)	P_{eff} = 0	20 000 6 096	14 700 4 481	-0.096	0.169	0.273	-0.159	2.65
Calcite crystal[12] (hexag. approx.)	P_{eff} = 0	17 500 5 334	11 000 3 353	0.369	0.127	0.579	0.169	2.71
Biotite crystal[12]	P_{eff} = 0	13 300 4 054	4 400 1 341	1.222	-1.437	-0.388	6.12	3.05
Apatite crystal[12]	P_{eff} = 0	20 800 6 340	14 400 4 389	0.097	0.257	0.586	0.079	3.218
Ice I crystal[12]	P_{eff} = 0, 4°F	11 900 3 627	5 500 1 676	-0.038	-0.10	-0.164	0.031	1.064
Aluminum-lucite[13] composite	clamped; oil between layers	9 410 2 868	4 430 1 350	0.97	-0.89	-0.09	1.30	1.86

[8]Kaarsberg, 1968
[9]Podio et al., 1968
[10]King, 1964
[11]Schock et al., 1974
[12]Simmons and Wang, 1971

Table 1. Continued

Sample	Conditions	V_P (f/s) (m/s)	V_S (f/s) (m/s)	ε	δ*	δ	γ	ρ(g/cm³)
"Sandstone-shale"[14]	hypothetical 50-50	9 871 3 009	5 426 1 654	0.013	-0.010	-0.001	0.035	2.34
"SS-anisotropic shale"[14]	hypothetical 50-50	9 871 3 009	5 426 1 654	0.059	-0.042	-0.001	0.163	2.34
"Limestone-shale"[14]	hypothetical 50-50	10 845 3 306	5 968 1 819	0.134	-0.094	0.000	0.156	2.44
"LS-anisotropic shale"[14]	hypothetical 50-50	10 845 3 306	5 968 1 819	0.169	-0.123	0.000	0.271	2.44
"Anisotropic shale"[14]	hypothetical 50-50	9 005 2 745	4 949 1 508	0.103	-0.073	-0.001	0.345	2.34
"Gas sand-water sand"[14]	hypothetical 50-50	4 624 1 409	2 560 780	0.022	-0.002	0.018	0.004	2.03
"Gypsum-weathered material"[14]	hypothetical 50-50	6 270 1 911	2 609 795	1.161	-1.075	-0.140	2.781	2.35

[13]Dalke, 1983
[14]Levin, 1979

that

$$\varepsilon = \frac{v_p(\pi/2) - \alpha_0}{\alpha_0} \tag{18b}$$

is, in fact, the fractional difference between vertical and horizontal P velocities, i.e., it is the parameter usually referred to as "the" anisotropy of a rock. [Without the factor of 2 in equation (8a), ε would not correspond to this common usage of the term "anisotropy."]

However, the parameter δ which controls the near-vertical anisotropy is a different combination of elastic moduli, which does not include C_{11} (i.e., the horizontal velocity) at all. Since the ε term is negligible for near-vertical propagation, most of one's intuitive understanding of ε is irrelevant to such problems. For example, it is normally true that horizontal P velocity is greater than vertical P velocity, i.e., $\varepsilon > 0$ (Table 1). However, this is of little use in understanding anisotropy in near-vertical reflection problems, because ε is multiplied by $\sin^4 \theta$ in equation (16a). The near-vertical anisotropic response is dominated by the δ term, and few can claim much intuitive familiarity with this combination of parameters [equation (17)]. In fact, Table 1 shows a substantial fraction of cases with negative δ.

Figures 2 and 3 show P wavefronts radiating from a point source into two uniform half-spaces, each with positive ε but different values of δ, one positive and one negative. These are just plots of $V_p(\phi)$ in polar coordinates. It is clear from the figures that quite complicated wavefronts may occur. Similar complications arise with SV wavefronts, although no actual cusps or triplications are present in the limit of weak anisotropy. (The term V_{NMO} in these figures is discussed in the next section.)

At this point, where the linearization procedure has identified δ as the crucial anisotropic parameter for near-vertical P-wave propagation, it is appropriate to discuss a special case of transverse isotropy which has received much attention: elliptical anisotropy. An elliptically anisotropic medium is characterized by elliptical P wavefronts emanating from a point source. It is defined (cf., Daley and Hron, 1979) by the condition

$$\delta = \varepsilon \qquad \ldots \text{elliptical anisotropy.}$$

Notable for its algebraic simplicity, this special case, is, of course, defined by a mathematical restriction of the parameters which has no physical justification. Accordingly, one may expect the occurrence of such a case in nature to be vanishingly rare. In fact, Table 1 shows that δ and ε are not even well-correlated (being frequently of opposite sign), so that the assumption of their equality may lead to serious error. This point is reinforced by Figure 4, which plots δ versus ε for the rocks of Table 1 and shows for comparison the elliptic condition defined above. The inadequacy of the elliptic assumption is immediately obvious.

These results are for intrinsic anisotropy. Berryman (1979) and Helbig (1979) show that if anisotropy is caused by fine layering of isotropic materials, then strictly

$$\delta < \varepsilon \qquad \ldots \text{isotropic layers.}$$

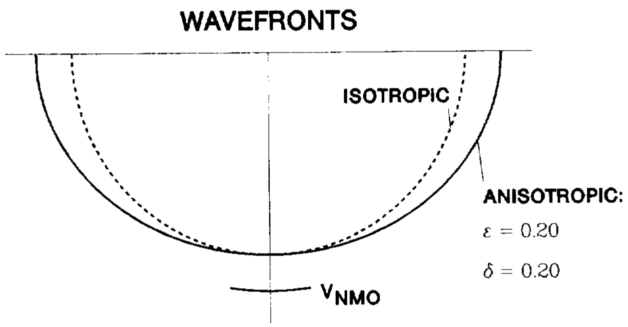

FIG. 2. This figure indicates an elliptical wavefront ($\delta = \varepsilon$). The curve marked V_{NMO} is a segment of the wavefront that would be inferred from isotropic moveout analysis of reflected energy. $V_{NMO} > V_{vert}$.

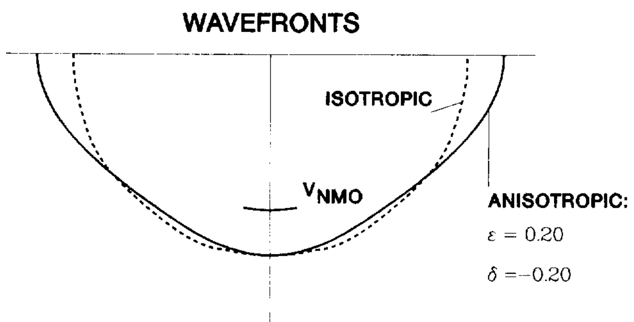

FIG. 3. This figure indicates a plausible anisotropic wavefront ($\delta = -\varepsilon$). The curve marked V_{NMO} is a segment of the wavefront that would be inferred from isotropic moveout analysis of reflected energy. $V_{NMO} < V_{vert}$ since $\delta < 0$.

As a final remark, note that, for small θ the last term in equation (16a), $\varepsilon \sin^4 \theta$, might be comparable to a neglected quadratic term in $\delta^2 \sin^2 \theta$, or $\delta\varepsilon \sin^2 \theta$. However, all neglected terms quadratic in anisotropy are multiplied by trigonometric terms of order $\sin^4 \theta \cos^4 \theta$ or smaller, and hence are in fact negligible, even for small θ.

Berryman (1979) writes a perturbation approximation to equation (10) in which the small parameter is a combination of anisotropic parameters and trigonometric functions. His derivation, which is also valid for strong anisotropy at small angles, reduces to the present equations (16a) and (16b) for weak anisotropy (at any angle). His approximation is less restrictive than the present one, but it yields formulas which are less simple (and which do not readily disclose the crucial role of the parameter δ, or contrast it with ε). It is therefore an approximation intermediate between the exact expressions (10) and the intuitively accessible approximation (16).

Backus (1965) treats the case of weak anisotropy of arbitrary symmetry, defining anisotropy differently than is done here, without implementing criteria (1) and (2) which follows equation (7d).

Consideration of the linearized SV result equation (16b) immediately confirms the well-known special result that elliptical P wavefronts ($\delta = \varepsilon$) imply spherical SV wavefronts (no θ dependence). However, equation (16b) shows that the more general case of weakly anisotropic but nonelliptical media is still algebraically tractable.

For completeness, note from equation (16c) that

$$\gamma = \frac{v_{SH}(\pi/2) - \beta_0}{\beta_0},$$

so that γ corresponds to the conventional meaning of "SH anisotropy." Also note that in the elliptical case $\delta = \varepsilon$, the functional form of equation (16a) becomes the same as that of equation (16c). This demonstrates that SH wavefronts are elliptical in the general case; this is true even for strong anisotropy.

Returning to the central point of δ as the crucial parameter in near-vertical anisotropic P-wave propagation, some discussion is necessary regarding the reliability of its measurement. It is clear from equations (16a) and (18b) that δ may be found directly (in the case of weak anisotropy) from a single set of measurements at $\theta = 0$, 45 and 90 degrees:

$$\delta = 4\left[V_p(\pi/4)/V_p(0) - 1\right] - \left[V_p(\pi/2)/V_p(0) - 1\right].$$

Because of the factor of 4, errors in $V_p(\pi/4)/V_p(0)$ propagate into δ with considerable magnification. In fact, if the relative standard error in each velocity is 2 percent, then the (independently) propagated absolute standard error in δ is of order .12, which is of the same order as δ itself (Table 1). The propagation of this error through equation (17) implies that the relative error in C_{13} is even larger. To reduce these errors to within acceptable limits requires many redundant experiments, of both $V_p(\theta)$ and $V_{SV}(\theta)$. Since the measurement at 45 degrees may involve cutting a separate core, questions of sample heterogeneity (as distinct from anisotropy) naturally arise. The data of Table 1 should be viewed with appropriate caution.

SOME APPLICATIONS OF WEAK ANISOTROPY

Group velocity

For the quasi-P-wave, the derivative in equation (14) is given for the case of weak anisotropy [equation (16a)] by

$$\frac{1}{v_p}\frac{\partial v_p}{\partial \theta} = \frac{2\alpha_0^2}{v_p^2(\theta)} \sin\theta \cos\theta \left[\delta + 2(\varepsilon - \delta)\sin^2\theta\right], \quad (19)$$

i.e., it is linear in anisotropy. Therefore, the group velocity [equation (14)] expanded in such terms,

$$V_p(\phi) = v_p(\theta)\left[1 + \frac{1}{2v_p^2}\left(\frac{\partial v_p}{\partial \theta}\right)^2\right],$$

is quadratic in anisotropy. Therefore, this term is neglected in the linear approximation

$$V_p(\phi) = v_p(\theta). \quad (20a)$$

Similarly for the other wave types,

$$V_{SV}(\phi) = v_{SV}(\theta); \quad (20b)$$

and

$$V_{SH}(\phi) = v_{SH}(\theta). \quad (20c)$$

Note that equations (20) do *not* say that group velocity equals phase velocity (or equivalently, that ray velocity equals wavefront velocity). These equations do say that at a given ray (group) angle ϕ, if the corresponding wavefront normal (phase) angle θ is calculated using equations (22) below, then equations (16) and (20) may be used to find the ray (group) velocity.

Group angle

The relationship (13) between group angle ϕ and phase angle θ is, in the linear approximation,

$$\tan \phi = \tan \theta \left[1 + \frac{1}{\sin \theta \cos \theta} \frac{1}{v(\theta)} \frac{dv}{d\theta} \right]. \qquad (21)$$

For P-waves, use of equation (19) (fully linearized) in equation (21) leads to

$$\tan \phi_p = \tan \theta_p \left[1 + 2\delta + 4(\varepsilon - \delta) \sin^2 \theta_p \right]. \qquad (22a)$$

Similarly, for SV-waves,

$$\tan \phi_{SV} = \tan \theta_{SV} \left[1 + 2 \frac{\alpha_0^2}{\beta_0^2} (\varepsilon - \delta)(1 - 2 \sin^2 \theta_{SV}) \right]; \qquad (22b)$$

and for SH-waves,

$$\tan \phi_{SH} = \tan \theta_{SH} (1 + 2\gamma). \qquad (22c)$$

These expressions, along with equations (16) and (20), define the group velocity, at any angle, for each wave type.

Note that inclusion of the anisotropy terms in the angles [equations (22)], when used in conjunction with the phase-velocity formulas [equation (16)], does not constitute a violation of the linearization process, even though products of small quantities implicitly appear. In linearizing equations (10) in terms of anisotropy, the angle θ was held constant, i.e., was not part of the linearization process. The linear dependence of θ on anisotropy, at fixed ϕ, is then given by equations (22).

Polarization angle

The particle motion of a quasi-P-wave is polarized in the direction of the eigenvector $\mathbf{g}_p$ (Daley and Hron, 1977), where

$$\mathbf{g}_p(\theta) = \ell_p \sin \theta_p \hat{\mathbf{x}} + m_p \cos \theta_p \hat{\mathbf{z}}. \qquad *$$

Since this is not parallel to the propagation vector $\mathbf{k}_p$ [equation (11)], the wave is said to be quasi-longitudinal, rather than strictly longitudinal; similar remarks apply to the quasi-SV-wave. The angle ζ_p between $\mathbf{k}_p$ and $\mathbf{g}_p$ is given by

$$\cos \zeta_p = \frac{1}{k_p g_p} (\mathbf{k}_p \cdot \mathbf{g}_p) = \frac{1}{k_p g_p} (\ell_p \sin^2 \theta_p + m_p \cos^2 \theta_p). \qquad *$$

Expressions for the scalars ℓ_p and m_p are given by Daley and Hron (1977); in the case of weak anisotropy, these expressions reduce to

$$\ell_p = 1 + \Delta \ell_p;$$

and

$$m_p = 1 + \Delta m_p,$$

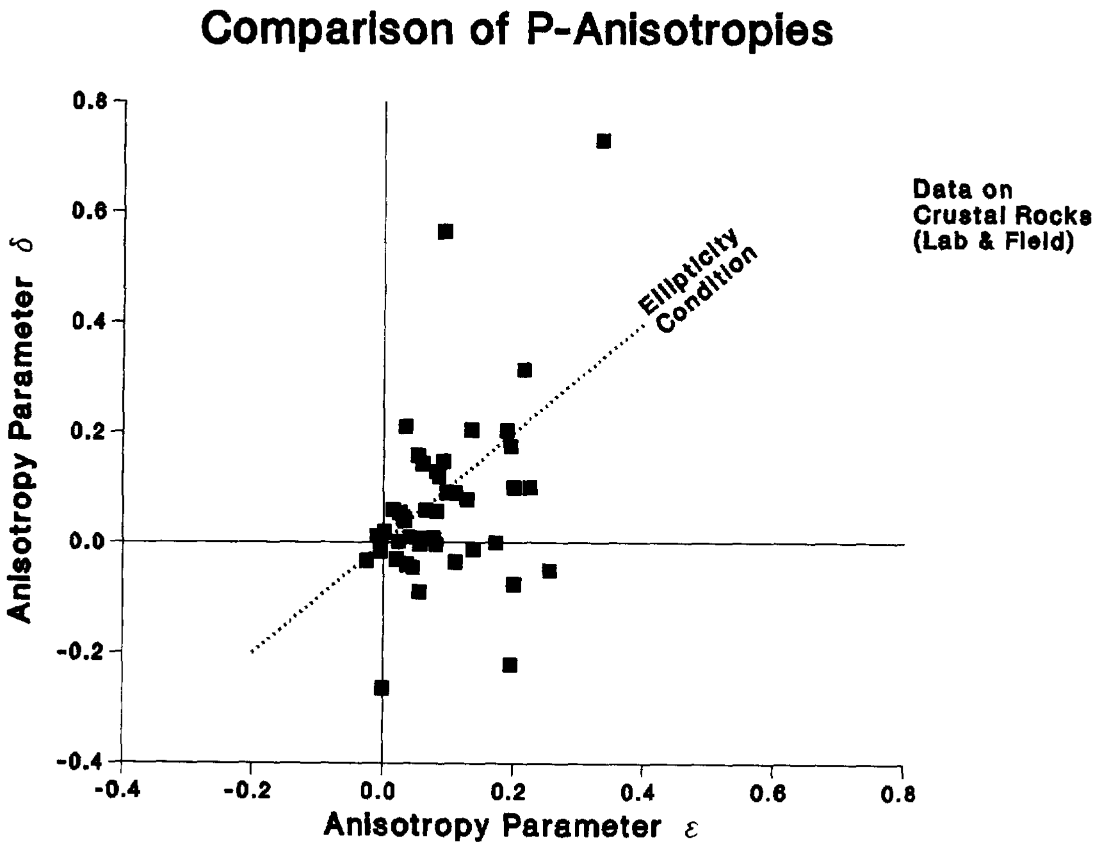

FIG. 4. This figure indicates the noncorrelation of the two anisotropy parameters δ and ε for the data in Table 1.

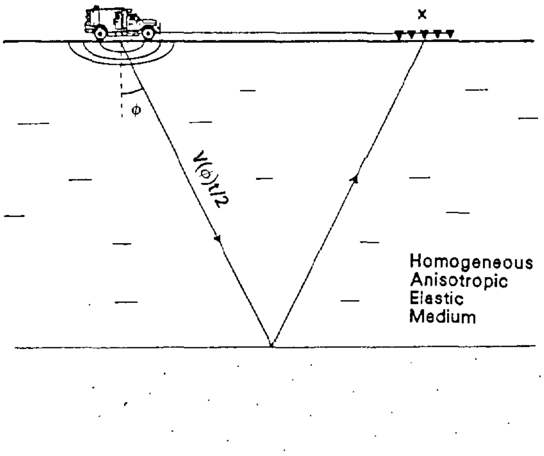

FIG. 5. A cartoon showing a simple reflection experiment through a homogeneous anisotropic medium.

where $\Delta \ell_p$ and Δm_p are linear in anisotropies ε and δ. It follows directly that

$$\cos \zeta_p = 1,$$

i.e., $\zeta_p = 0$, and in the linear approximation the departure of the polarization direction $\mathbf{g}_p$ from the wave vector $\mathbf{k}_p$ is negligible. Of course, $\mathbf{g}_p$ deviates from the *ray* by the amount defined in equation (22a). This conclusion appears to disagree with a result by Backus (1965).

Corresponding remarks apply to the shear polarization vectors; they are each transverse to the corresponding $\mathbf{k}$, in the case of weak anisotropy. The polarization of each S-wave deviates from the normal to the *ray* direction by the amount defined in equation (22b).

Moveout velocity

Consider a homogeneous anisotropic layer through which a conventional reflection survey is performed (Figure 5). The raypath to any offset $x(\phi)$ consists of two straight segments, as shown in the figure. The traveltime t is given (trivially) as

$$\left[V(\phi)\frac{t(\phi)}{2}\right]^2 = \left[V(0)\frac{\tau}{2}\right]^2 + \left(\frac{x}{2}\right)^2, \qquad *$$

where τ is the vertical traveltime. Solving for t^2,

$$t^2(\phi) = \left[\frac{V(0)}{V(\phi)}\right]^2 \left[\tau^2 + \frac{x^2}{V^2(0)}\right]. \qquad (23)*$$

Because of the ϕ dependence, the function in equation (23) plots along a curved line (instead of a straight line) in the $t^2 - x^2$ plane. The slope of this line is

$$\frac{dt^2}{dx^2} = \frac{1}{V^2(\phi)} - \frac{t^2}{V^2}\frac{dV^2}{dx^2}$$
$$= \frac{1}{V^2(\phi)}\left[1 - \frac{2\cos^2\phi}{V(\phi)}\frac{dV(\phi)}{d\sin^2\phi}\right]. \qquad (24)*$$

Normal-moveout velocity is defined using the initial slope of this line:

$$\frac{1}{V_{\mathrm{NMO}}^2} \equiv \lim_{x\to 0}\left(\frac{dt^2}{dx^2}\right) = \frac{1}{V^2(0)}\left[1 - \frac{2}{V(0)}\frac{dV(\phi)}{d\sin^2\phi}\right]_0. \qquad (25)*$$

(This is, of course, the short-spread V_{NMO}.) The second term on the right is generally not zero. Hence it is clear from equation (25) that, even in the limit of small x offsets (i.e., with all waves propagating nearly vertically), with all velocities near $V(0)$, the resulting moveout velocity is not the vertical velocity $V(0)$.

Carrying out the derivative [using equation (13)] is algebraically tedious, but straightforward. For P-waves, the derivation is

$$V_{\mathrm{NMO}}(P) = \alpha_0\sqrt{1 + 2\delta}, \qquad (26a)*$$

independent of ε. The value of this velocity is indicated in Figures 2 and 3 by a short arc below the origin. This line represents a segment of that "wavefront" which would be inferred by an isotropic analysis of a surface reflection experiment such as that depicted in Figure 5.

For SV-waves,

$$V_{\mathrm{NMO}}(SV) = \beta_0\left[1 + 2\frac{\alpha_0^2}{\beta_0^2}(\varepsilon - \delta)\right]^{1/2}; \qquad (26b)*$$

for SH-waves (which have elliptical wavefronts)

$$V_{\mathrm{NMO}}(SH) = \beta_0\sqrt{1 + 2\gamma}$$
$$= v_{SH}(\pi/2) = V_{SH}(\pi/2). \qquad (26c)*$$

The last result (for SH) does not require the limit $x \to 0$, i.e., the $t^2 - x^2$ graph is a straight line, as for isotropic media. This is a well-known result for elliptical wavefronts (Van der Stoep, 1966), as is the fact that the resulting V_{NMO} is identical to the horizontal velocity, even though all rays are near-vertical.

For weak anisotropy, equations (26) reduce to

$$V_{\mathrm{NMO}}(P) = \alpha_0(1 + \delta); \qquad (27a)$$

$$V_{\mathrm{NMO}}(SV) = \beta_0\left[1 + \frac{\alpha_0^2}{\beta_0^2}(\varepsilon - \delta)\right]; \qquad (27b)$$

and

$$V_{\mathrm{NMO}}(SH) = \beta_0(1 + \gamma). \qquad (27c)$$

Comparison of equations (27a) and (18a) shows that, for P-waves, the moveout velocity is equal to neither the vertical velocity α_0 nor the horizontal velocity $\alpha_0(1 + \varepsilon)$. Neither is the moveout velocity necessarily intermediate between these two values, since δ and ε may be of opposite sign (Table 1).

Equation (26a) is equivalent to expression (3) of Helbig (1983). In the present version, the departure of $V_{\mathrm{NMO}}/\alpha_0$ from unity is clearly related to the same anisotropic parameter δ which appears so prominently in other applications.

Horizontal stress

One way to estimate the horizontal stress in the sedimentary crust of the Earth is to describe an element of rock at depth as a linearly elastic medium in uniaxial strain (Hubert and Willis, 1957). Despite the obvious shortcomings of this approximation (e.g., the difference between static and dynamic moduli, Lin, 1985), it remains widely used as a means to estimate horizontal stress for hydrofracture control, etc.

The analysis is normally done in terms of isotropic media; it is instructive to consider the same problem in anisotropic media. Here, "anisotropy" still is taken to mean "transverse isotropy with symmetry axis vertical," even though this sort of analysis is usually done in a context of preferred horizontal stress direction, resulting in an oriented hydrofracture. This may often be justified, since the resulting azimuthal anisotropy is usually of the order of 1–2 percent, whereas the conventional anisotropy is frequently 10–20 percent.

The vertical stress σ_{33} and the horizontal stress σ_{11} are, from equation (1), related by

$$\sigma_{33} = C_{31}\varepsilon_{11} + C_{32}\varepsilon_{22} + C_{33}\varepsilon_{33} \tag{28a}$$

and

$$\sigma_{11} = C_{11}\varepsilon_{11} + C_{12}\varepsilon_{22} + C_{13}\varepsilon_{33}. \tag{28b}$$

The other strain terms vanish because of null values of $C_{\alpha\beta}$. (In the application to hydrofracturing, these stresses are replaced by effective stresses; however, the following argument is not affected.)

In the case of uniaxial strain, $\varepsilon_{11} = \varepsilon_{22} = 0$, so that the horizontal stress is

$$\sigma_{11} = \sigma_{33}\frac{C_{13}}{C_{33}}. \tag{29}$$

The vertical stress is due to gravity:

$$\sigma_{33} = -\rho g z,$$

where g is the acceleration due to gravity and z is the depth. In the isotropic case, the ratio of elastic moduli [equation (4)] may be expressed in several equivalent ways:

$$\frac{\sigma_{11}}{\sigma_{33}} = \frac{C_{13}}{C_{33}} = \frac{\lambda}{\lambda + 2\mu} = \frac{\nu}{1-\nu} = \frac{K - \frac{2}{3}\mu}{K + \frac{4}{3}\mu} = 1 - 2\frac{\beta^2}{\alpha^2}, \tag{30}$$

where α and β are the velocities of P-waves and S-waves, respectively, and ν is Poisson's ratio. Hence, α and β could be measured in situ and, given the assumptions just stated, σ_{11} could be estimated using equations (29)–(30).

In the anisotropic case, the corresponding expression is, from equation (17),

$$\frac{\sigma_{11}}{\sigma_{33}} = \frac{C_{13}}{C_{33}} = \left(1 - 2\frac{\beta_0^2}{\alpha_0^2}\right) + \left(1 - \frac{\beta_0^2}{\alpha_0^2}\right)\left\{\left[1 + 2\delta\Big/\left(1 - \frac{\beta_0^2}{\alpha_0^2}\right)\right]^{1/2} - 1\right\}. \tag{31*}$$

For weak anisotropy, equation (31) reduces to

$$\frac{\sigma_{11}}{\sigma_{33}} = \frac{C_{13}}{C_{33}} = \left(1 - 2\frac{\beta_0^2}{\alpha_0^2}\right) + \delta. \tag{32}$$

Comparison with the last formulation of equation (30) shows that the anisotropic correction is given simply by the anisotropy parameter δ. In a typical case, $\beta_0/\alpha_0 \approx 0.5$, so that the first term in equation (32) is also ≈ 0.5. Table 1 shows that δ is often not negligible in comparison to 0.5; the correction may be either positive or negative. Therefore, use of the isotropic model, equation (30), may lead to serious overestimates or underestimates of horizontal stress [equation (29)]. These errors may reinforce or reduce errors due to failure of other aspects of the model of elastic uniaxial strain.

DISCUSSION

The casual term "the anisotropy" of a rock usually means the quantity ε, calculated using equation (18b). It is often implied that, if ε and the vertical velocity α_0 are known, the velocity at oblique angles is calculable simply by using some trigonometric relations. Of course, this assumption is not true; the P velocity at oblique angles requires knowledge of a third physical parameter, in addition to the trigonometric functions. Equation (16a) shows that, for weakly anisotropic media, the relevant third parameter is the anisotropic parameter δ. The equation further shows that, for near-vertical P-wave propagation, the δ contribution completely dominates the ε contribution. Because of this, δ (rather than ε) controls the anisotropic features of most situations in exploration geophysics, including the relationships among ray angles, wavefront angles, and polarization angles and the moveout velocity for P-waves, and the horizontal stress-overburden ratio.

With today's computers, there is little excuse for using the linearized equations (16) for computational purposes, even when the anisotropy is so small that their numerical accuracy is high. All programs should be written using the exact equations (10) or (7). The linearized equations are useful because their simplicity of form aids in the understanding of the physics. For example, in a forward modeling program, a routine may be able to "predict data" for comparison with real data that seem to call for an anisotropic interpretation. A primary obstacle is that few geophysicists are prepared to propose reasonable values for the five different $C_{\alpha\beta}$ required by the program, or to adjust values iteratively to match the real data. However, most interpreters can propose reasonable values of vertical velocities α_0 and β_0 from direct experience with isotropic ideas. Further, most are prepared to estimate the values of anisotropies ε (and γ if needed); the sign (+) and general magnitude (0–20 percent) are commonplace. That leaves only δ (for a P or SV problem), and the linearized equations (16) imply that determination of δ is where iterative adjustments should be concentrated, since the value of δ is probably the most crucial. Table 1 illustrates its range of values, extending into both the positive and negative ranges.

Table 1 also provides a guide for construction, for modeling purposes, of an equivalent anisotropic medium from finely layered isotropic media. A tempting simplification is to assume a constant Poisson's ratio among these isotropic layers (Levin, 1979). It is easy to show analytically (Backus, 1962), as verified numerically in the corresponding entries of Table 1, that assumption of constant Poisson's ratio leads to $\delta = 0$. While this value is indeed plausible, nonzero values of either sign are also plausible. This particular choice happens to minimize the resultant anisotropic effects for P-waves. The assumption of constant Poisson's ratio is, therefore, a dangerous one. The hypothetical sequences shown in Table 1 should not be taken as representative for any actual area without careful justification. (These comments are entirely consistent with those of Thomas and Lucas, 1977, and of course with the calculations of Levin, 1979.)

A second point that deserves further emphasis is that "weak" anisotropy (defined as $\varepsilon, \delta, \gamma \ll 1$), by definition, leads to second-order corrections whenever the anisotropy is compared to unity, as in equations (16). However, the anisotropy sometimes occurs in a context where it is comparable, not to unity, but to another small number [e.g., equation (32)]. In this case, the anisotropy makes a first-order contribution, rather than a second-order correction (even though it is defined as weak), and should therefore not be neglected. Other common contexts of interest in exploration geophysics where the anisotropy appears in this way as a first-order effect will be the subject of future contributions.

ACKNOWLEDGMENTS

I thank C. S. Rai, A. L. Frisillo, J. A. Kelley (of Amoco Production Company), and W. Lin (of Lawrence Livermore Laboratory) for permission to publish their data (Table 1) in advance of its public appearance under their own names. I thank A. Seriff (of Shell) for useful comments.

REFERENCES

Backus, G. E., 1962, Long-wave elastic anisotropy produced by horizontal layering: J. Geophys. Res., **67**, 4427–4440.
——— 1965, Possible forms of seismic anisotropy of the uppermost mantle under oceans: J. Geophys. Res., **70**, 3429.
Berryman, J. G., 1979, Long-wave elastic anisotropy in transversely isotropic media: Geophysics, **44**, 896–917.
Daley, P. F., and Hron, F., 1977, Reflection and transmission coefficients for transversely isotropic media: Bull., Seis. Soc. Am., **67**, 661–675.
——— 1979, Reflection and transmission coefficients for seismic waves in ellipsoidally anisotropic media: Geophysics, **44**, 27–38.
Dalke, R. A., 1983, A model study: wave propagation in a transversely isotropic medium: M.Sc. thesis, Colorado School of Mines.
Helbig, K., 1979, Disucssion on "The reflection, refraction and diffraction of waves in media with elliptical velocity dependence" by F. K. Levin: Geophysics, **44**, 987–990.
——— 1983, Elliptical anisotropy—Its significance and meaning: Geophysics, **48**, 825–832.
Hubbert, M. K., and Willis, D. B., 1957, Mechanics of hydraulic fracture: Trans., Am. Inst. Min. Metallurg. Eng., **210**, 153–166.
Jones, E. A., and Wang, H. F., 1981, Ultrasonic velocities in Cretaceous shales from the Williston basin: Geophysics, **46**, 288–297.
Kaarsberg, E. A., 1968, Elastic studies of isotropic and anisotropic rock samples: Trans., Am. Inst. Min. Metallurg. Eng., **241**, 470–475.
Keith, C. M., and Crampin, S., 1977a, Seismic body waves in anisotropic media: Reflection and refraction at a plane interface: Geophys. J. Roy. Astr. Soc., **49**, 181–208.
——— 1977b, Seismic body waves in anisotropic media: Propagation through a layer: Geophys. J. Roy. Astr. Soc., **49**, 209–224.
——— 1977c, Seismic body waves in anisotropic media: Synthetic seismograms: Geophys. J. Roy. Astr. Soc., **49**, 225–243.
King, M. S., 1964, Wave velocities and dynamic elastic moduli of sedimentary rocks: Ph.D. thesis, Univ. of California at Berkeley.
Kelley, J. A., 1983, Amoco Production Company: Private communication (Table 1).
Krey, T. H., and Helbig, K., 1956, A theorem concerning anisotropy of stratified media and its significance for reflection seismics: Geophys. Prosp., **4**, 294–302.
Levin, F. K., 1979, Seismic velocities in transversely isotropic media: Geophysics, **44**, 918–936.
Lin, W., 1985, Ultrasonic velocities and dynamic elastic moduli of Mesaverde rock: Lawrence Livermore Nat. Lab. Rep. 20273, rev. 1.
Nye, J. F., 1957, Physical properties of crystals: Oxford Press.
Podio, A. L., Gregory, A. R., and Gray, M. E., 1968, Dynamic properties of dry and water-saturated Green River shale under stress: Soc. Petr. Eng. J., **8**, 389–404.
Rai, C. S., and Frisillo, A. L., 1982, Amoco Production Company: Private communication (Table 1).
Robertson, J. D., and Corrigan, D., 1983, Radiation patterns of a shear-wave vibrator in near-surface shale: Geophysics, **48**, 19–26.
Schock, R. N., Bonner, B. P., and Louis, H., 1974, Collection of ultrasonic velocity data as a function of pressure for polycrystalline solids: Lawrence Livermore Nat. Lab. Rep. UCRL-51508.
Simmons, G., and Wang, H., 1971, Single crystal elastic constants and calculated aggregate properties: A handbook: Mass. Inst. Tech. Press.
Thomas, J. H., and Lucas, A. L., 1977, The effects of velocity anisotropy on stacking velocities and time-to-depth conversion: Geophys. Prosp., **25**, 583.
Tosaya, C., 1982, Acoustical properties of clay-bearing rocks: Ph.D.. thesis, Stanford Univ.
Van der Stoep, D. M., 1966, Velocity anisotropy measurements in wells: Geophysics, **31**, 900–916.
White, J. E., Martineau-Nicoletis, L., and Monash, C. 1982, Measured anisotropy in Pierre shale: Geophys. Prosp., **31**, 709–725.